

Surface Deformation Analysis by Fusion of Multi-temporal and Multi-source Data under Disaster Emergency Conditions

Anpeng Shen¹, Shuangfeng Wei¹, Yuanyuan Wang², Zhaodong Yang³, Shouxin Zhu⁴

¹ Beijing University of Civil Engineering and Architecture, 102616 Beijing, China - 2108570022130@stu.bucea.edu.cn, weishuangfeng@bucea.edu.cn

² Shaoxing Bureau Of Natural Resources and Planning, 312000 Shaoxing, China - 39590233@qq.com

³ Shaoxing Huayuan Land Survey Co., Ltd., 312000 Shaoxing, China - 52746134@qq.com

⁴ Shaoxing Geotechnical Investigation & Surveying Institute, 312000 Shaoxing, China - 1229126297@qq.com

Keywords: Emergency Surveying & Mapping, Multi-temporal Data, Multi-source Remote Sensing Data, Data Fusion, Surface Deformation Analysis.

Abstract

Rapid analysis of surface deformation is crucial for rescue operations following natural disasters. However, the lack of recent terrain data and the discrepancy between data types and field-collected data often hinder timely surface deformation analysis. To enhance data usability, this paper proposes an analytical method that integrates multiple sources of remote sensing data, including satellite data, oblique photography data, and LiDAR data. By merging oblique images with grayscale point clouds, true-color point clouds are generated. The method optimizes old data through threshold segmentation and median filtering, then converts and unifies the resolution of multi-source data via data interpolation. Elevation interpolation matrices are employed for overlay analysis, and a combination of bilateral filtering and threshold processing is used. This groundbreaking approach enables the completion of surface deformation analysis in emergency geospatial surveys and has been validated in various typical regions, demonstrating its application potential across different surface environments. Experimental results indicate that this method can quickly utilize multi-temporal and multi-source remote sensing data to effectively identify surface deformations following natural disasters.

1. Background

In the current context of globalization, the frequent occurrence of natural disasters poses a great challenge to human society. Disasters not only cause loss of life and property, but also have a profound impact on regional economic development. Moreover, there is an optimal time period for disaster relief, and in order to save as many lives as possible, it is especially important to quickly and accurately analyze the surface deformation caused by natural disasters.

Emergency mapping after natural disasters is the basic support for all kinds of public emergencies to provide geographic information and modern surveying and mapping technology, is an important part of the national emergency response system, is the command decision-making and rescue and disaster relief guarantee and basis, is through the whole process of public emergencies prevention, response, disposal and restoration of the importance of the basic work.

Disaster analysis relies on multi-period topographic data, so it is necessary to obtain multi-period data from previous periods and the scene. By comparing the multi-period data and analyzing the information such as surface subsidence is the main analysis method at present (Zheng, et al., 2022). Firstly, historical data often present numerous challenges. For instance, in remote mountainous regions, past terrain data may have been collected manually due to the absence of UAVs and other advanced equipment, resulting in poor data quality due to outdated cartographic techniques. Furthermore, in emergency surveying scenarios, the high demands for speed and timeliness mean that, even if high-precision data are available from other sources, field personnel often do not have the time to obtain them and must rely on the historical data they have at hand. Additionally, due to technological limitations and communication difficulties, it is challenging to obtain externally transmitted data at disaster sites.

At the disaster site, in order to facilitate situational awareness, emergency responders need instant access to maps of the site (Opach, et al., 2023). Conventional methods typically involve manual investigation within the disaster zone, which is not only inefficient and limited in scope but also exposes responders to the risks of secondary hazards.

Combining drones with various sensors offers the advantages of rapid, automated, and non-contact spatial data collection, providing high resolution and accuracy (Kovanič, et al., 2023). In recent years, UAV remote sensing has gradually attracted the attention of scientific researchers and industry, due to its broad application prospects. It has been widely used in agriculture, forestry, mining, and other industries. UAVs can be flexibly equipped with various sensors, such as optical, infrared, and LIDAR, and become an essential remote sensing observation platform (Zhang, et al., 2023). Consequently, they are commonly used in emergency surveying scenarios. UAV remote sensing methods produce more detailed maps, which can expedite rescue and relief operations in disaster-affected areas (Singh, et al., 2023).

Furthermore, the long intervals between multiple datasets mean that the sensors used for data collection at disaster sites may differ from those used in historical data. This results in highly complex multi-temporal and multi-source data scenarios in emergency surveying, increasing the difficulty of terrain analysis and often causing delays in rescue operations. The most common application of drones is their effective creation of spatial models based on photogrammetry and LiDAR data (Kovanič, et al., 2023). UAV Light Detection Ranging (UAV-LiDAR) and UAV photogrammetry are currently common ground monitoring techniques (Zhan, et al., 2024).

Photogrammetry stands out for its mobility, flexibility, and intuitiveness, particularly its ability to visually represent disaster

scenes through color models, aiding in swift assessment and disaster relief coordination. However, in areas with vegetation cover such as forests, photogrammetry is limited by its passive measurement nature, which cannot penetrate the vegetation layer to directly obtain surface data (Kim, et al., 2023). UAV-mounted LiDAR, with its continuous operation and high-precision data, is widely used in terrain surveying and 3D modeling (Jiang, et al., 2022). In complex terrains such as forests, LiDAR technology, with its high precision and active measurement capabilities, excels in vegetation penetration through multi-echo technology, allowing it to directly obtain accurate surface data. In extreme environments, such as snow-covered forests, UAV-mounted LiDAR can effectively provide information about both the canopy and the sub-canopy snow surface (Koutantou, et al., 2022). Despite these advantages, the grayscale point clouds produced by LiDAR lack true color and texture information, limiting their application in disaster site assessment. Previous studies have alternated between these two technologies, overlooking their correlation, or have compared them solely on an individual basis (Zhan, et al., 2024). Combining the advantages of these two technologies through multi-sensor data

fusion has become an urgent need to enhance disaster relief efficiency.

In summary, emergency surveying is a crucial component of the emergency response system for public incidents, providing geographic information support and decision-making foundations. Faced with the complexity of disaster sites, the key challenge is how to rapidly and comprehensively utilize multi-temporal, multi-source remote sensing data to resolve surface deformation analysis difficulties and provide both intuitive and high-precision visual data. Traditional methods are inefficient and pose secondary disaster risks. By integrating multi-temporal and multi-sensor data, it is possible to enhance disaster relief efficiency, achieve rapid and accurate surface deformation analysis, and optimize the overall effectiveness of emergency surveying.

2. Methodology

To address these challenges, this paper proposes an innovative method. The technical approach is illustrated in Figure 1.

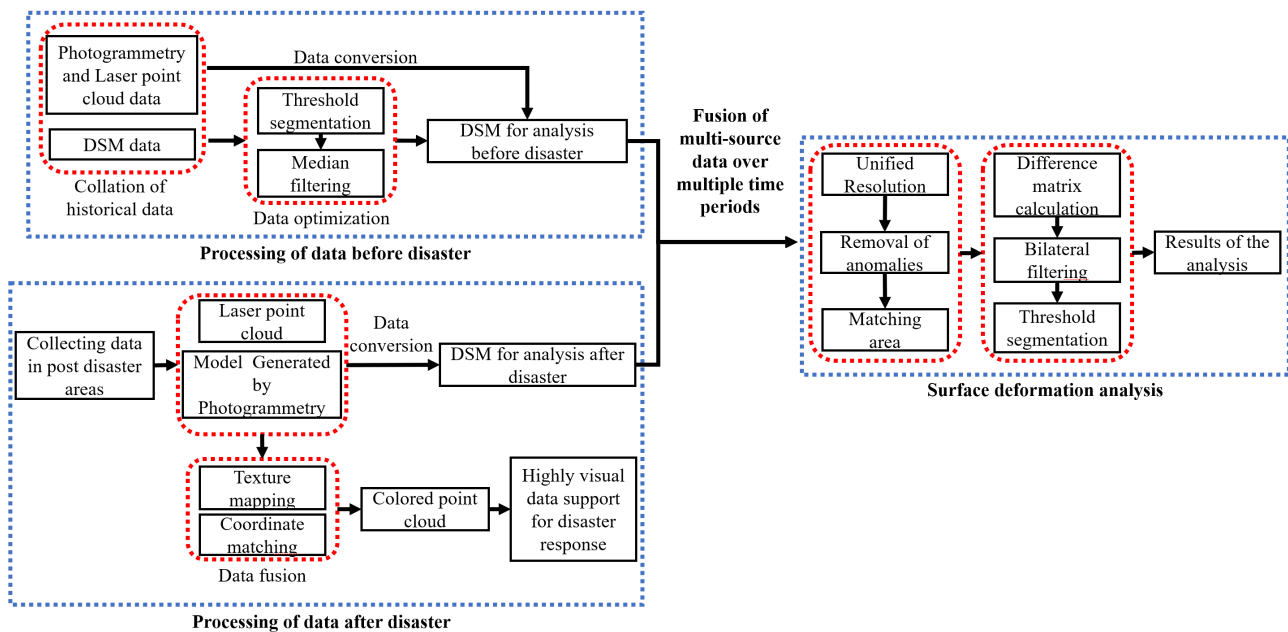


Figure 1. Technology approach.

The entire roadmap is divided into three main sections: processing of data before disaster, processing of data after disaster, and surface deformation analysis. The analysis process also includes the step of generating true-color point clouds. This method comprehensively utilizes multiple data sources such as satellite imagery, photogrammetry, and LiDAR. Through a series of technical processing steps, it not only optimizes old data but also effectively integrates data from different sources to enhance the speed of surface deformation analysis.

The pre-disaster data collected from the database is optimized using methods such as threshold segmentation and median filtering, primarily aimed at improving data in anomalous areas and enhancing the accuracy of subsequent analysis. For post-disaster on-site data, nearest-neighbor coordinate matching and texture mapping are used to merge photogrammetric data with LiDAR point cloud data, producing true-color point clouds. The multi-source data is then converted into DSM models, enabling

the integration of various types of pre-disaster and on-site collected data.

Considering the differences in data from different time periods, data interpolation is used to unify the resolution, followed by geographic coordinate matching for regional alignment. The processed multi-source, multi-temporal data undergoes overlay analysis using elevation interpolation matrices. Techniques such as bilateral filtering and threshold processing further optimize the results. Experimental validation in multiple typical regions demonstrates the method's effectiveness and practicality.

2.1 Raw Data Preprocessing

In emergency surveying, the quality of historical data often presents issues, making the rapid processing of raw data essential. One of the most common problems is the presence of anomalies in elevation data.

For data before disaster, optimization is carried out using methods such as threshold segmentation and median filtering. The specific process is illustrated in Figure 2.

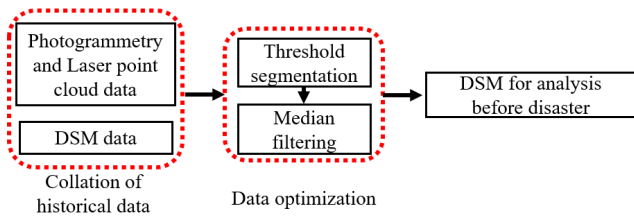


Figure 2. Processing of data before disaster.

Firstly, since surface data falls within a normal range, threshold segmentation is initially used to screen the data. This step identifies anomalies such as elevation issues, effectively isolating data points that do not conform to natural terrain variation characteristics, thereby laying the foundation for further processing. Further, the median filtering algorithm is applied for data optimization. A median filter is a nonlinear filter that eliminates digital signal noise while preserving signal edges. This technique has been widely used in two-dimensional digital filtering. It involves selecting an odd-numbered template window, moving it along the rows or columns of the two-dimensional digital matrix, and replacing the values within the window with the median value (An, et al., 2024).

The formula for the median filter used in this paper is shown in Equation 1:

$$g(x, y) = \text{median}\{f(x - i, y - j)\}, (i, j) \in S, \quad (1)$$

where $f(x, y)$ = preprocessed pixel matrix
 $g(x, y)$ = the post-processing pixel matrix
 S = window area

The larger the template for median filtering, the more noise is filtered out. However, the deviation of the center value of the template window from the observed value can lead to wrong results. Therefore, a 3*3 template is used for filtering in this paper. The median filtering schematic is shown in Figure 3.

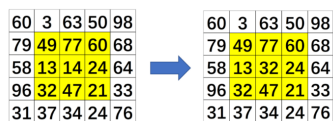


Figure 3. Schematic diagram of the median filter principle.

Regardless of whether the area is flat or a complex mountainous region, terrain data should exhibit good continuity between ground points on a global scale. The median filtering method is highly effective at removing extremely high or low anomalous points in continuous terrain, while preserving terrain features and edge information. This achieves optimization of data in anomalous regions.

2.2 True Color Point Cloud Generation

In disaster scenes, high-precision data that allows for intuitive assessment of surface deformation is extremely valuable. The fusion of 3D LiDAR point clouds with 2D imagery is a current

research hotspot in the field of photogrammetry and remote sensing.

By combining the high precision of 3D LiDAR point clouds with the high observability of 2D image texture data, on-site personnel can quickly assess the disaster situation.

The 3D model obtained from oblique photogrammetry is converted into a Digital Orthophoto Map (DOM). Since the current data has the same geographic coordinate system, matching the same regions becomes possible, forming the basis for data fusion. Then, the converted DOM and the LiDAR-derived LAS format files are merged using nearest-neighbor coordinate matching and texture mapping. This process integrates the photogrammetric data with the LiDAR point cloud data, resulting in the output of true-color point clouds.

Specifically, the converted DOM files and LAS files are used to extract pixel data and point cloud data, respectively. After extraction, the two types of data are matched using the nearest-neighbor method based on their coordinates. Post-matching, the point cloud is processed to attach the texture from the image data to the grayscale point cloud. Finally, this results in the output of true-color point clouds, achieving the goal of multi-sensor data fusion.

Moreover, since the reference factor for texture attachment is the geographic coordinate system, there is no need for joint calibration of the multi-sensors involved in the fusion. As long as the coordinate systems of the original data are consistent, the fusion process can be realized. This characteristic significantly enhances data production efficiency in post-disaster emergency surveying scenarios where timeliness is critical.

2.3 Surface Deformation Analysis

In disaster sites where rapid surface deformation analysis is required, the diversity of raw data types can negatively impact the workflow. Therefore, it is necessary to integrate multi-temporal, multi-sensor, and multi-source data to lay the foundation for data analysis.

To standardize satellite imagery data, oblique measurement data, and LiDAR point cloud data into a unified format, a series of processing and standardization steps are essential. By converting multi-source data into DSM models, we achieve the integration of various types of data from pre- and post-disaster scenes over multiple time periods.

Subsequently, the integrated multi-temporal, multi-sensor, and multi-source data undergo surface deformation analysis. The specific technical approach is illustrated in Figure 4.

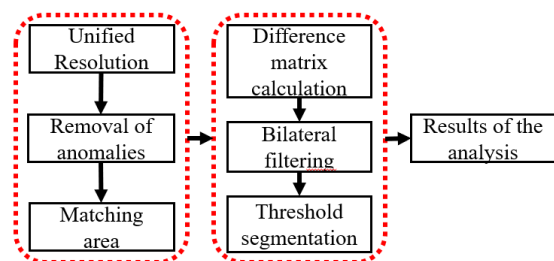


Figure 4. Processing of data before disaster.

The process is mainly divided into three parts: data preprocessing, surface deformation analysis, and result output. Firstly, considering the different resolutions of various data, we unify the data resolution through interpolation. Anomalous points are then removed using threshold analysis and median filtering, as described in Equation 1. Geographic coordinates are used to match the regions, preventing discrepancies due to varying extents of the original data from affecting the analysis results. Next, elevation difference matrices are used to analyze the same locations across multiple datasets. The results are optimized using bilateral filtering. In practical surface deformation analysis, minute deformations may be disregarded, so thresholding is applied to extract areas that have undergone significant changes. These extracted areas represent the disaster-affected regions. Finally, the surface deformation analysis results are generated.

The calculation formula for extracting elevation information at the same location from two-period DSM data in the same region is shown in Equation 2:

$$\Delta H_{i,j} = H_2(i,j) - H_1(i,j) \quad i = 1 \dots M, j = 1 \dots N, \quad (2)$$

where $H(i, j)$ = the elevation value of data
 $\Delta H(i, j)$ = the elevation difference of data
 M = location ranges
 N = location ranges

By reading the elevation information from two-period DSM data, we perform pixel-by-pixel elevation differencing to obtain the difference DSM elevation matrix.

The entire experimental area is traversed, and the elevation differences in the DSM data are calculated to form the elevation difference matrix. The size of the elevation difference matrix, like the experimental area of the DSM data, is $M \times N$. The elevation difference matrix is shown in Equation 3:

$$dH = \begin{pmatrix} \Delta H_{11} & \dots & \Delta H_{1N} \\ \vdots & \ddots & \vdots \\ \Delta H_{M1} & \dots & \Delta H_{MM} \end{pmatrix}, \quad (3)$$

If H_{ij} is less than 0, the location is an elevation decrease point. If H_{ij} is larger than 0, it means that the location is an elevation increase point. Difference DSM data information is easily affected by the accuracy of DSM data before and after the time-phase, so when using DSM data to extract the change information, the elevation threshold t can be set.

If the absolute value of the extracted elevation difference is greater than t and the elevation difference is positive, the grid point is considered an elevation increase point. If the absolute value of the extracted elevation difference is less than t and the elevation difference is negative, the grid point is considered an elevation decrease point. If the absolute value of the extracted elevation difference equals t , it is considered unchanged information.

Bilateral filtering is a nonlinear filter used in image processing to remove noise, such as Gaussian noise, while preserving edges. This effect is achieved through two main functions: determining the filter coefficient based on geometric spatial distance and the difference between adjacent grid values. In the bilateral filtering algorithm, the output grid value is a weighted combination of adjacent grid values.

It combines both spatial proximity and pixel value similarity to smooth the image while preserving edge information. This filter

reduces image noise while avoiding the edge blurring problems commonly associated with traditional filtering methods such as Gaussian filtering.

In the bilateral filtering algorithm, the output grid value is a weighted combination of adjacent grid values. The ability of the bilateral filter to smooth noise while preserving edges is due to its filter kernel being generated by two functions: the kernel domain and the value range kernel.

The kernel domain, the template weights $d(i, j, k, l)$ determined by the Euclidean distance of the pixel positions, is shown in Equation 4:

$$d(i, j, k, l) = \exp\left(-\frac{(i-k)^2 + (j-l)^2}{2\sigma_d^2}\right), \quad (4)$$

Value range kernel, determined by the difference in pixel values, assigns weights to the template values $r(i, j, k, l)$. The specific formula is shown in Equation 5:

$$r(i, j, k, l) = \exp\left(-\frac{\|f(i, j) - f(k, l)\|^2}{2\sigma_r^2}\right), \quad (5)$$

where (i, j) = the grid position
 (k, l) = the range centered on (i, j) $(2N+1)(2N+1)$
 $f(k, l)$ = the grid value involved in the calculation
 σ_d^2 = the variance of the grid position distance
 σ_r^2 = the variance of the grid value

Multiplying the two templates gives the template weights of the bilateral filter, is shown in Equation 6:

$$w(i, j, k, l) = \exp\left(-\frac{(i-k)^2 + (j-l)^2}{2\sigma_d^2} - \frac{\|f(i, j) - f(k, l)\|^2}{2\sigma_r^2}\right), \quad (6)$$

Therefore, the data equation for the bilateral filter can be expressed as Equation 7:

$$g(i, j) = \frac{\sum_{k,l} f(k, l) w(i, j, k, l)}{\sum_{k,l} w(i, j, k, l)}, \quad (7)$$

Considering the difference between the value domain and the air domain, compared with the difference between the traditional Gaussian filter or the mean filter of a single spatial domain and/or value domain, it can better remove noise while retaining characteristics (An, et al., 2024).

By using the above methods, different sensor data can be fused, and the required DSM can be obtained from the data acquired by various sensors. Processing the data from multiple periods and different sensors allows for detailed surface elevation difference analysis. This comparison can reveal surface changes such as landslides, ground subsidence, and other deformations.

3. Experiments

An experiment was conducted to validate the optimization method for historical data proposed in this paper. The experimental results are shown in Figure 5.

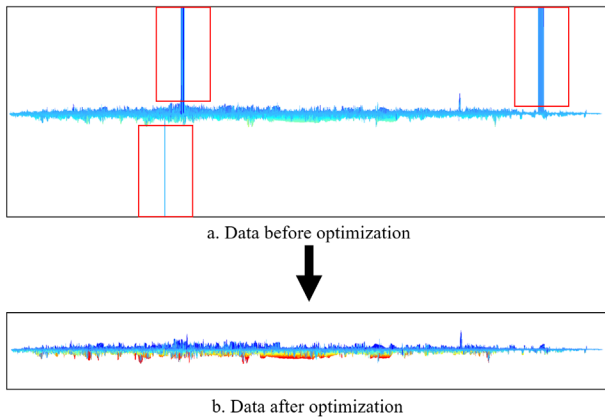


Figure 5. Optimization results of problem data.

Figure a shows the acquired historical data, where clear anomalies can be observed due to earlier collection methods and time periods. Figure b presents the optimized results, where the previously evident anomalies have been successfully mitigated.

The median filtering method is highly effective at removing extremely high or low anomalous points in continuous terrain, while preserving terrain features and edge information. By comparing the data before and after optimization, the experimental results demonstrate that this method effectively eliminates anomalous regions in the data.

Subsequently, to verify the feasibility and applicability of achieving true-color point clouds through data fusion, typical regions were selected for the true-color point cloud generation experiment. The results are shown in Figure 6.

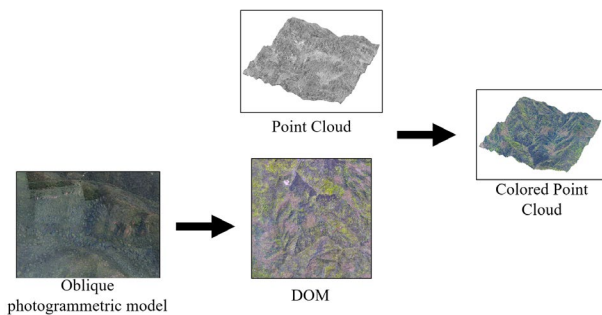


Figure 6. Generation of colored point cloud.

The main process involves converting the oblique model obtained from photogrammetry into a Digital Orthophoto Map (DOM) and fusing it with LiDAR point cloud data that only contains grayscale information, resulting in the output of true-color point clouds with color texture.

Oblique photography and LiDAR data collection are conducted in the selected area, ensuring that both data sets share a consistent geographic coordinate system. Then, the collected data undergoes denoising, filtering, and format conversion to ensure data quality.

The photographic data is processed to generate the DOM. Since the geographic coordinate systems are consistent, the nearest-neighbor coordinate matching method can be used to attach the color texture information from the DOM to the grayscale LiDAR

point cloud. This fusion technique produces true-color point clouds.

The integration of multiple sensors, such as cameras and LiDAR, successfully provides intuitive and high-precision visual data for disaster relief efforts.

Finally, to validate the feasibility and applicability of the surface deformation analysis techniques proposed in this paper, we conducted analyses in mining and industrial areas. By processing and analyzing data from these typical regions, we confirmed the overall scheme and algorithm's feasibility and applicability. The experimental process and results are shown in Figure 7.

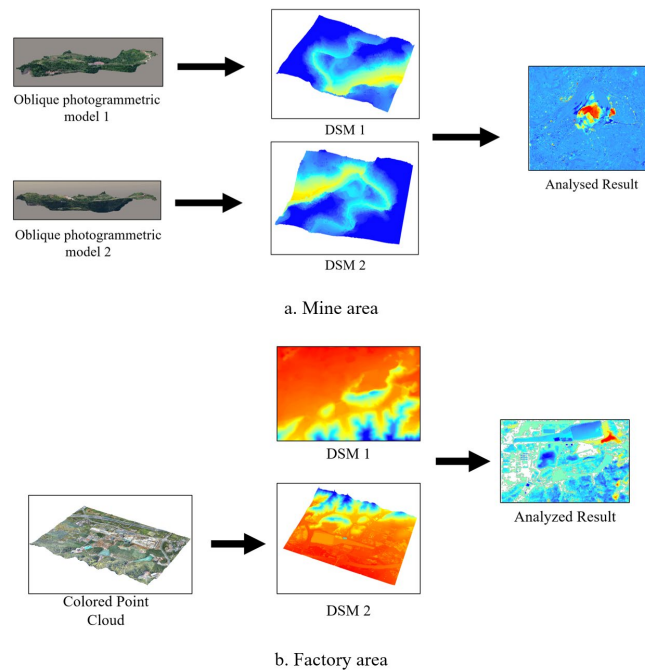


Figure 7. Typical area experiment.

Figure a shows the analysis conducted in the mining area, while Figure b illustrates the analysis in the industrial area. In Figure a, the analysis of models obtained from two periods of oblique photogrammetry successfully yielded surface deformation results. In Figure b, surface deformation analysis was achieved by combining the previously generated true-color point cloud data with historical DSM data.

Data collection was carried out in both mining and urban areas, including oblique photography and LiDAR scanning. The collected raw data was processed and converted into the appropriate formats. Using the preprocessed data, true-color point clouds were generated, and DSMs were subsequently created. By employing comparative analysis techniques, the surface deformation in both areas was assessed.

Mining areas typically have complex terrain and significant surface changes, providing an ideal environment for testing the effectiveness of techniques in analyzing subsidence and other geological activities. Urban areas, with dense buildings and varied surface changes due to construction, traffic development, and other factors, test the method's application in highly complex and dynamically changing environments.

To evaluate the accuracy and precision of the methods proposed in this paper, multiple elevation points within the experimental areas were measured using GPS-RTK. The analysis results were then compared with the data obtained from GPS-RTK measurements. The comparison results are shown in Table 1:

Measure points	Observatory data	Analyzed data	Error
1	16.592 m	16.644 m	0.052 m
2	16.642 m	16.609 m	-0.033 m
3	17.705 m	17.753 m	0.048 m
4	17.658 m	17.689 m	0.031 m
5	17.121 m	17.084 m	-0.037 m

Table 1. Results validation data

The error range is between 0.031m and 0.052m, with a difference of less than 0.06m, and a standard deviation of 0.039m. These results meet the practical accuracy requirements for surface deformation detection. This outcome validates the effectiveness and practicality of our research methods, confirming that the results fully satisfy the demands of real-world applications.

4. Conclusion

This paper proposes a method for surface deformation analysis under disaster emergency conditions by integrating multi-temporal and multi-source data. The method aims to quickly and accurately assess surface changes caused by natural disasters, providing reliable support for rescue decision-making.

The main contributions of this paper are as follows:

In the context of globalization, frequent natural disasters pose significant challenges to human society. Post-disaster emergency surveying is fundamental to rescue efforts, and quickly obtaining accurate information on terrain changes is crucial for saving lives and property.

This paper proposes a comprehensive analytical method that integrates satellite imagery, oblique photogrammetry, and LiDAR data. Through true-color point cloud generation, data preprocessing, and surface deformation analysis, effective integration and rapid analysis of multi-source data are achieved.

Historical data are optimized using threshold segmentation and median filtering to enhance data quality. Oblique imagery and LiDAR point clouds are fused to generate point cloud data with true colors and textures. Elevation interpolation matrices and bilateral filtering techniques are employed to perform multi-temporal data overlay analysis and extract surface deformation information.

Experiments conducted in multiple typical regions validate the method's potential for application in various surface environments. The results demonstrate that the method can quickly apply multi-temporal, multi-source remote sensing data to effectively identify surface deformations following natural disasters.

This method significantly improves the efficiency and accuracy of post-disaster emergency surveying, providing strong support for emergency response and disaster relief decision-making. By integrating multi-source remote sensing data, it optimizes data

utilization and analytical flexibility, offering new perspectives and tools for future disaster response and other applications.

This study offers an innovative solution for surface deformation analysis, holding significant practical implications and application prospects in the field of emergency surveying.

Acknowledgement

This work is supported by the Shaoxing Municipal Bureau of Natural Resources and Planning Production Project (CGSHZJ-2023-N000849).

References

- Zheng, J., Yao, W., Lin, X., Ma, B., Bai, L., 2022. An accurate digital subsidence model for deformation detection of coal mining areas using a UAV-based LiDAR. *Remote Sensing* 14, 421.
- Opach, T., Rød, J.K., Munkvold, B.E., 2023. Map functions to facilitate situational awareness during emergency events. *Cartography and Geographic Information Science* 50, 546–561.
- Kovanič, L., Topitzer, B., Pet'ovský, P., Blišťan, P., Gergel'ová, M.B., Blišťanová, M., 2023. Review of photogrammetric and Lidar applications of UAV. *Applied Sciences* 13, 6732.
- Zhang, Z., Zhu, L., 2023. A review on unmanned aerial vehicle remote sensing: Platforms, sensors, data processing methods, and applications. *Drones* 7, 398.
- Singh, C.H., Jain, K., Mishra, V., 2023. UAV-Based Terrain-Following Mapping Using LiDAR in High Undulating Catastrophic Areas, in: Jain, K., Mishra, V., Pradhan, B. (Eds.), *Proceedings of UASG 2021: Wings 4 Sustainability*, Lecture Notes in Civil Engineering. Springer International Publishing, Cham, pp. 21–37.
- Zhan, X., Zhang, X., Wang, X., Diao, X., Qi, L., 2024. Comparative analysis of surface deformation monitoring in a mining area based on UAV-lidar and UAV photogrammetry. *The Photogrammetric Record* phor.12490.
- Kim, J., Kim, I., Ha, E., Choi, B., 2023. UAV Photogrammetry for Soil Surface Deformation Detection in a Timber Harvesting Area, South Korea. *Forests* 14, 980.
- Jiang, N., Li, H.-B., Li, C.-J., Xiao, H.-X., Zhou, J.-W., 2022. A fusion method using terrestrial laser scanning and unmanned aerial vehicle photogrammetry for landslide deformation monitoring under complex terrain conditions. *IEEE Transactions on Geoscience and Remote Sensing* 60, 1–14.
- Koutantou, K., Mazzotti, G., Brunner, P., Webster, C., Jonas, T., 2022. Exploring snow distribution dynamics in steep forested slopes with UAV-borne LiDAR. *Cold Regions Science and Technology* 200, 103587.
- An, S., Yuan, L., Xu, Y., Wang, X., Zhou, D., 2024. Ground subsidence monitoring in based on UAV-LiDAR technology: a case study of a mine in the Ordos, China. *Geomech. Geophys. Geo-energ. Geo-resour.* 10, 57.